Fast Computer Vision based Geometry Estimation

Bachelor Thesis

Authors
Cédric Renda, Manuel Tischhauser
Supervisor
Prof. Dr. Guido M. Schuster
Subject
Image Processing

HSR Hochschule Für Technik Rapperswil
May 15, 2020

Abstract

Introduction

Approach

Conclusion

Contents

Abbreviations

RMS Root Mean Square

Chapter 1

Introduction

Chapter 2

Theory

This chapter takes a closer look at the theory and technology applied in this thesis.

2.1 Camera Calibration in OpenCV

Camera calibration is needed to obtain camera parameters like focal length and center point. Further, it provides a method to correct distortions caused by the imperfect optics according to a certain distortion models. For that, images of a known pattern (usually a checkerboard) have to be taken from different view-points an angles. These points provide the training data which is needed to estimate all the coefficients.

This section describes the theory behind the calibration process in OpenCV. Subsections 2.1.1 and 2.1.2 adapt the parts of the theory and notation from the OpenCV 4.3.0 documentation **cv_calib**, which is the latest version at the time of writing this thesis.

2.1.1 The pinhole camera model

The functions OpenCV provides to calibrate the camera use the so-called pinhole camera model. This model describes, how a 3D-point specified in world-coordinates (P_w) is transformed to a 3D-point in camera-coordinates (P_c) and then further projected onto the image plane (p). After this step, the point is described as a 2D-point in pixel coordinates. Figure **??** illustrates this setup.

The transition from the world-coordinates to the camera-coordiantes can be described as

$$\underbrace{\begin{pmatrix} X_c \\ Y_c \\ Z_c \end{pmatrix}}_{P_c} = \underbrace{\begin{pmatrix} r_{11} & r_{12} & r_{13} \\ r_{21} & r_{22} & r_{23} \\ r_{31} & r_{32} & r_{33} \end{pmatrix}}_{R} \underbrace{\begin{pmatrix} X_w \\ Y_w \\ Z_w \end{pmatrix}}_{P_w} + \underbrace{\begin{pmatrix} t_x \\ t_y \\ t_z \end{pmatrix}}_{t} .$$

The vector P_w is first rotated by R and the translated by t. This can be written in one single matrix:

$$\begin{pmatrix} X_c \\ Y_c \\ Z_c \end{pmatrix} = \begin{pmatrix} r_{11} & r_{12} & r_{13} & t_x \\ r_{21} & r_{22} & r_{23} & t_y \\ r_{31} & r_{32} & r_{33} & t_z \end{pmatrix} \begin{pmatrix} X_w \\ Y_w \\ Z_w \\ 1 \end{pmatrix} \quad \Leftrightarrow \quad P_c = \begin{pmatrix} R & | & t \end{pmatrix} \begin{pmatrix} P_w \\ 1 \end{pmatrix}. \tag{2.1}$$

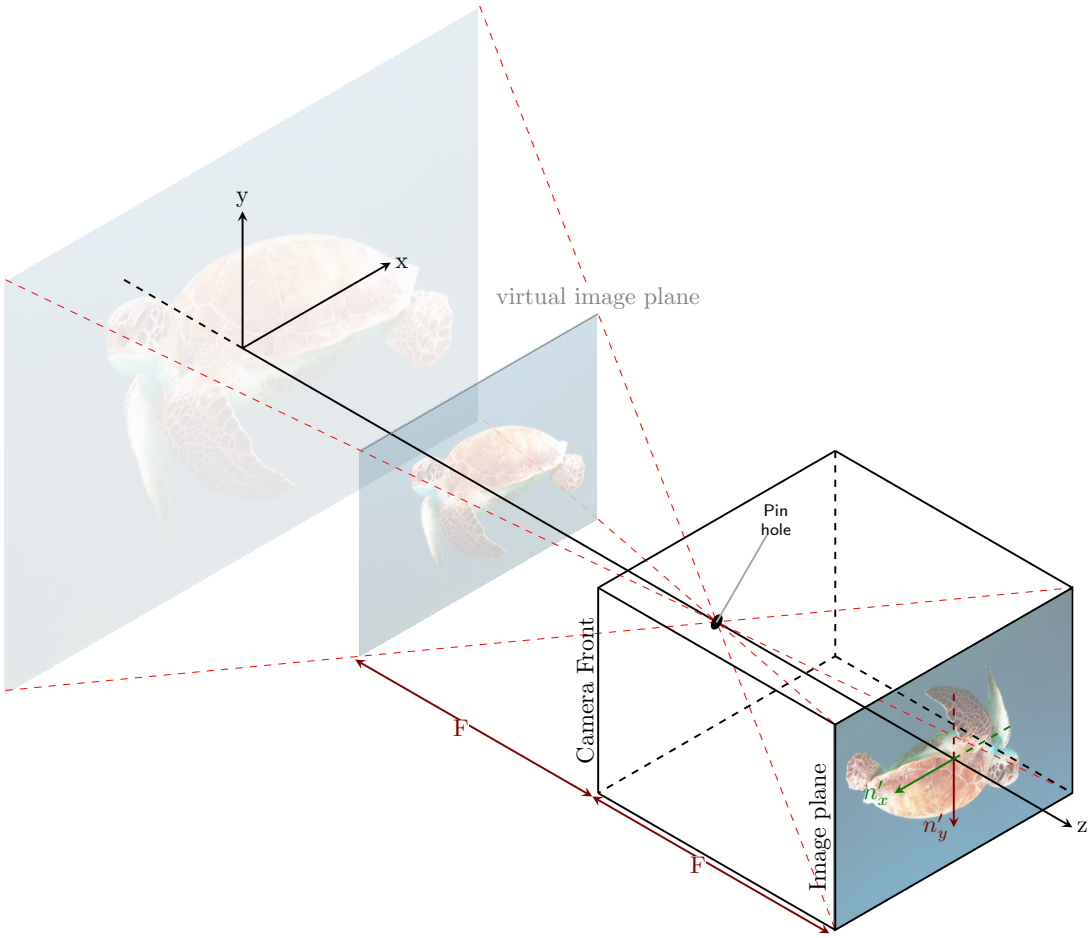

Figure 2.1: Pinhole-model whole camera.

As a result of the theorem of intersecting lines, the projection from P_c to p is described as

$$\underbrace{\begin{pmatrix} u \\ v \end{pmatrix}}_{p} = \begin{pmatrix} f_x \cdot X_c/Z_c \\ f_y \cdot y_c/Z_c \end{pmatrix} + \begin{pmatrix} c_x \\ c_y \end{pmatrix}.$$

where f_x and f_y are the focal length f (in world units) normalized by their respective pixel size (in world units). Thus f_x and f_y are the same, if the pixels are quadratic.

By adding the principal point $\begin{pmatrix} c_x & c_y \end{pmatrix}^T$, which is usually close to the image center, it is taken into account, that pixel-coordinates are specified with respect to the upper left corner of the image plane. . It is now simpler to write this in homogeneous coordinates:

$$\begin{pmatrix} u \\ v \\ 1 \end{pmatrix} \sim s \begin{pmatrix} u \\ v \\ 1 \end{pmatrix} = \underbrace{\begin{pmatrix} f_x & 0 & c_x \\ 0 & f_y & c_y \\ 0 & 0 & 1 \end{pmatrix}}_{K} \begin{pmatrix} X_c \\ Y_c \\ Z_c \end{pmatrix} \quad \Leftrightarrow \quad s \begin{pmatrix} p \\ 1 \end{pmatrix} = K \cdot P_c, \tag{2.2}$$

where s is an arbitrary scaling factor and K is called the camera matrix. The overall transition

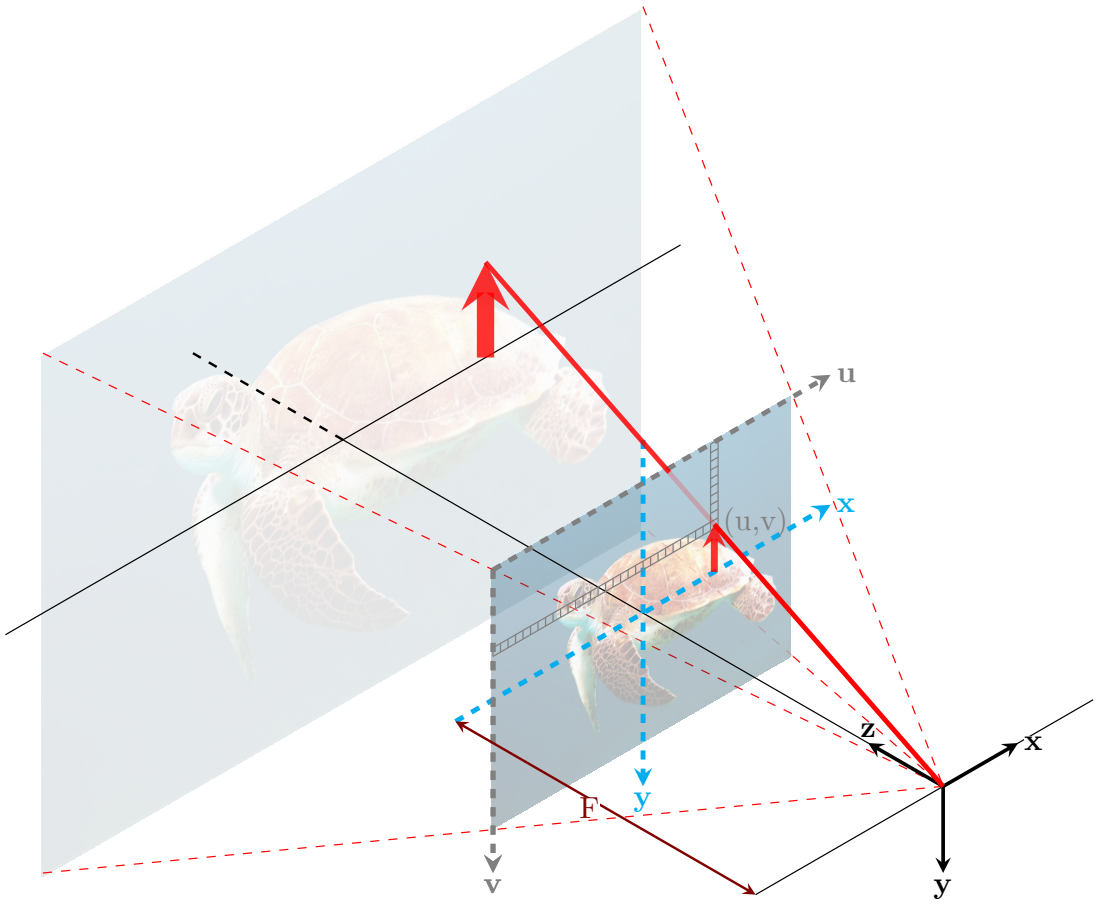

Figure 2.2: Pinhole-model simple model.

from world- to pixel-coordinates is the result of combining 2.1 and 2.2:

$$s\begin{pmatrix} u \\ v \\ 1 \end{pmatrix} = \begin{pmatrix} f_x & 0 & c_x \\ 0 & f_y & c_y \\ 0 & 0 & 1 \end{pmatrix} \begin{pmatrix} r_{11} & r_{12} & r_{13} & t_x \\ r_{21} & r_{22} & r_{23} & t_y \\ r_{31} & r_{32} & r_{33} & t_z \end{pmatrix} \begin{pmatrix} X_w \\ Y_w \\ Z_w \\ 1 \end{pmatrix} \quad \Leftrightarrow \quad s\begin{pmatrix} p \\ 1 \end{pmatrix} = K\begin{pmatrix} R & | & t \end{pmatrix}\begin{pmatrix} P_w \\ 1 \end{pmatrix} \tag{2.3}$$

The rotation and translation in $\begin{pmatrix} R & | & t \end{pmatrix}$ are called the extrinsic parameters. The camera matrix K contains analogously the linear intrinsic parameters.

2.1.2 The distortion model in OpenCV

Non linear distortions, which appear before the projection in 2.2 should be considered too. OpenCV takes the effects of radial, tangential and thin prism distortion into account.

Radial Distortion

Radial distortion is caused by the flawed curvature of the lens **weng**. It can be modeled with

$$\begin{pmatrix} x'' \\ y'' \end{pmatrix} = \begin{pmatrix} x' \frac{1+k_1 r^2+k_2 r^4+k_3 r^6}{1+k_4 r^2+k_5 r^4+k_6 r^6} \\ y' \frac{1+k_1 r^2+k_2 r^4+k_3 r^6}{1+k_4 r^2+k_5 r^4+k_6 r^6} \end{pmatrix}, \tag{2.4}$$

where x' and y' are coordinates, described in camera-coordinates, normalized with Z_c

$$\begin{pmatrix} x' \\ y' \end{pmatrix} = \begin{pmatrix} X_c/Z_c \\ Y_c/Z_c \end{pmatrix}$$

from and r is the radius as taken with respect to the principal point $\begin{pmatrix} c_x & c_y \end{pmatrix}^T$

$$r^2 = x'^2 + y'^2.$$

This type of distortion is symmetrical about the optical axis. Figure 2.3 illustrates the effect on a rectangle.

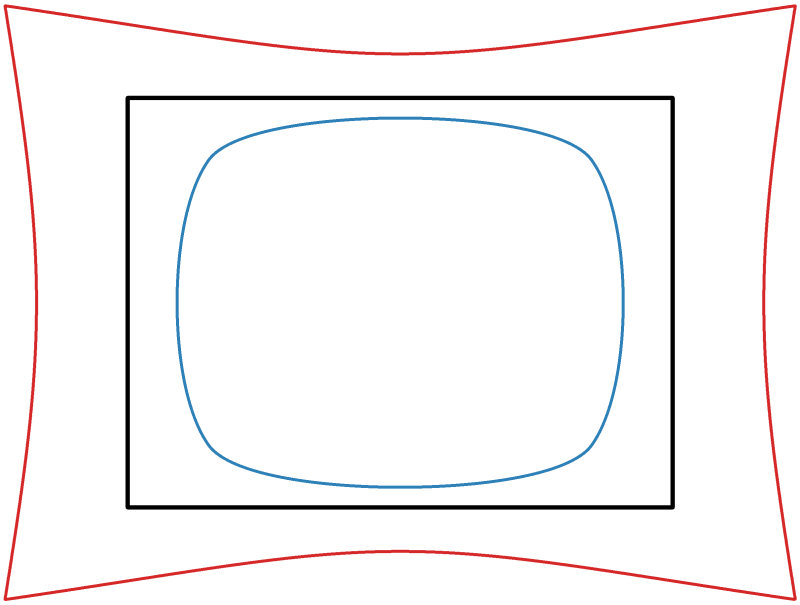

Figure 2.3: Different types of radial distortion. Black: no distortion, red: $k_1 = 10$, $k_2 = 11$, $k_3 = 12$, $k_4 = 5$, $k_5 = 6$, $k_6 = 7$, blue: $k_1 = -2.2$, $k_2 = -1.2$, $k_3 = -0.8$, $k_4 = -0.4$, $k_5 = -0.3$, $k_6 = -0.2$

Tangential distortion

Real optical systems are also subject to tangential distortion. This type of distortion has a decentering effect and occurs, if the line through the optical center of the lens and the principal point is not col-linear with the optical axis **weng**. The model

$$\begin{pmatrix} x'' \\ y'' \end{pmatrix} = \begin{pmatrix} x' + 2p_1x'y' + p_2(r^2 + 2x'^2) \\ y' + 2p_2x'y' + p_1(r^2 + 2y'^2) \end{pmatrix} \tag{2.5}$$

takes this into account. Figure 2.4 shows the distortion this model introduces.

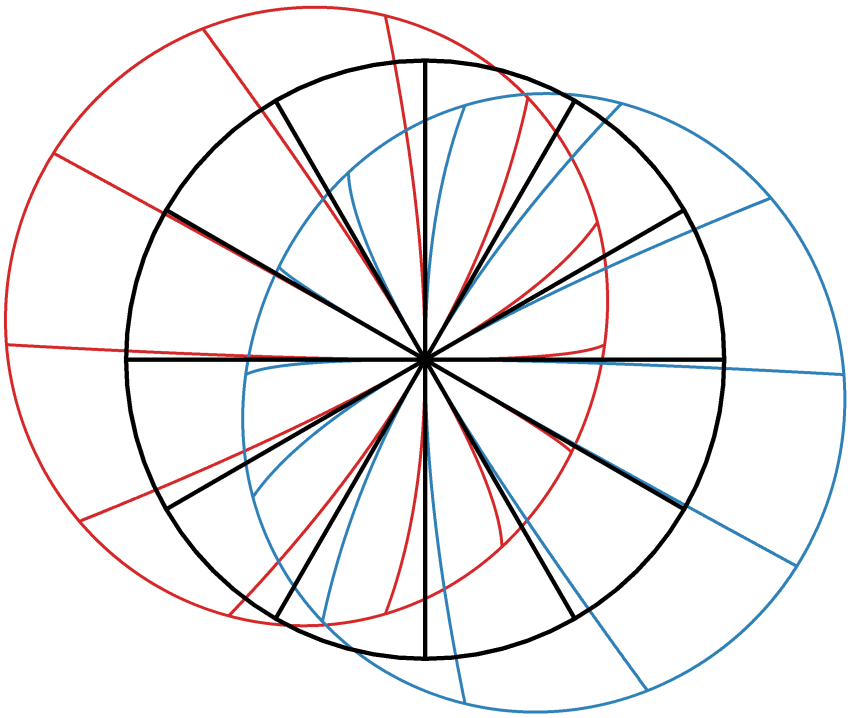

Figure 2.4: Different types of tangential distortion (example adapted from **weng**). Black: no distortion, red: $p_1 = -0.15$, $p_2 = -0.4$, blue: $p_1 = 0.15$, $p2 = -0.4$

Thin prism distortion

Thin prism distortion is partially caused by lens imperfections and camera assembly **weng**. It introduces additional radial and tangential distortion, modeled with

$$\begin{pmatrix} x'' \\ y'' \end{pmatrix} = \begin{pmatrix} x' + s_1 r^2 + s_2 r^4 \\ y' + s_3 r^2 + s_4 r^4 \end{pmatrix}. \tag{2.6}$$

The combined model in OpenCV

The models in 2.4, 2.5 and 2.6 combined result in

$$\begin{pmatrix} x'' \\ y'' \end{pmatrix} = \begin{pmatrix} x' \frac{1+k_1 r^2+k_2 r^4+k_3 r^6}{1+k_4 r^2+k_5 r^4+k_6 r^6} + 2p_1 x' y' + p_2(r^2 + 2x'^2) + s_1 r^2 + s_2 r^4 \\ y' \frac{1+k_1 r^2+k_2 r^4+k_3 r^6}{1+k_4 r^2+k_5 r^4+k_6 r^6} + 2p_2 x' y' + p_1(r^2 + 2y'^2) + s_3 r^2 + s_4 r^4 \end{pmatrix}. \tag{2.7}$$

In summary, a point in normalized camera-coordinates $\begin{pmatrix} x' & y' \end{pmatrix}^T$ is distorted as modeled in 2.7, which leads to the point $\begin{pmatrix} x'' & y'' \end{pmatrix}^T$. To get the distorted pixel-coordinates (subscript d), the projection has to be applied

$$\begin{pmatrix} u_d \\ v_d \end{pmatrix} = \begin{pmatrix} x'' f_x + c_x \\ y'' f_y + c_y \end{pmatrix} \quad \Leftrightarrow \quad \begin{pmatrix} u_d \\ v_d \\ 1 \end{pmatrix} = K \begin{pmatrix} x'' \\ y'' \\ 1 \end{pmatrix},$$

which completes the model so far. Keep in mind, that when correcting the distortion, equation 2.7 has to be inverted.

2.1.3 Reprojection error

The reprojection error is a value to asses the quality of a calibration. It is the error between the detected image point and the projection (using the obtained coefficients) of its corresponding world point onto the image plane. Since it only uses the points, which where previously used to obtain the calibration-parameters, it can be interpreted as a training error rate.

Calibration functions in OpenCV return the overall RMS reprojection error **cv_calib**.

2.1.4 Error propagation as further quality assessment

As argued before, the reprojection error is a training error rate. A low reprojection error is therefore not necessarily enough to estimate, how good the calibration really performs.

OpenCV returns with its extended calibration functions not only the camera intrinsics, but also an estimated standard deviation of each coefficient **cv_calib**. Under assumption that low standard deviations suggest a good calibration, it is valid to combine all standard deviations into one value using the propagation of uncertainty.

The propagation of error states that influence of each error of the inputs x_i on the output value y of a function

$$y = f(x_1, x_2, .., x_n)$$

can be linearly approximated and summed up to **benno**:

$$\Delta y = \sqrt{\sum_{i=1}^{n} \left(\frac{\partial y}{\partial x_i} \Delta x_i \right)^2}. \tag{2.8}$$

Applied to 2.7, this leads to

$$\Delta x'' = \sqrt{\sum_{i=1}^{6} \left(\frac{\partial x''}{\partial k_i} \Delta k_i \right)^2 + \sum_{i=1}^{2} \left(\frac{\partial x''}{\partial p_i} \Delta p_i \right)^2 + \sum_{i=1}^{4} \left(\frac{\partial x''}{\partial s_i} \Delta s_i \right)^2}$$

and

$$\Delta y'' = \sqrt{\sum_{i=1}^{6} \left(\frac{\partial y''}{\partial k_i} \Delta k_i \right)^2 + \sum_{i=1}^{2} \left(\frac{\partial y''}{\partial p_i} \Delta p_i \right)^2 + \sum_{i=1}^{4} \left(\frac{\partial y''}{\partial s_i} \Delta s_i \right)^2}.$$

It is at this point not intended to go into further computations of the derivatives. If we look at pixel coordinates from the center of the image, btw. $c_x = 0$ and $c_y = 0$, the radius (distance from the centerpoint) can be expressed as

$$r = \sqrt{(f_x \cdot x'')^2 + (f_y \cdot y'')^2}$$

and therefore, if errors in f_x and f_y are neglected, with the propagation in 2.8 applied

$$\Delta r = \sqrt{\left(\frac{\partial r}{\partial x''} \Delta x'' \right)^2 + \left(\frac{\partial r}{\partial y''} \Delta y'' \right)^2}. \tag{2.9}$$

This value Δr can now be plotted over half the diagonal of an image to compare calibration coefficients of different calibration approaches.

2.2 Measurement with back-light illumination

To measure the size and form of an object there are multiple ways. A popular way to get the contour is to place a light source behind the object desired to measure, and aim on the object with an camera. With this method the optical sensors get the silhouette of the object.

2.2.1 Light source

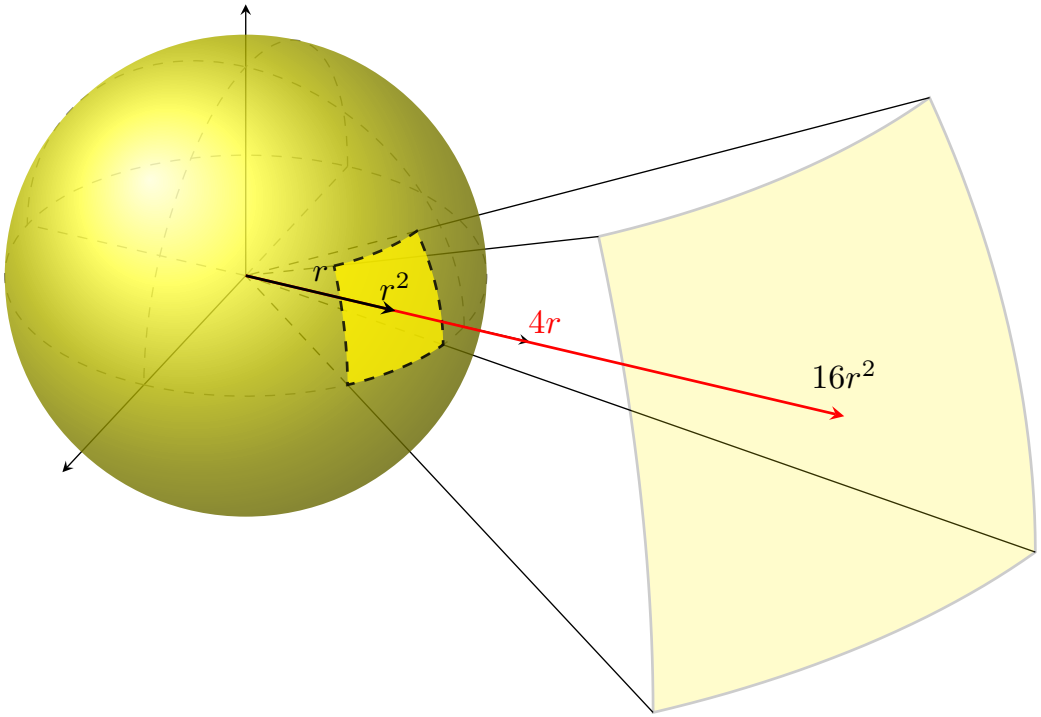

Figure 2.5: Light source in 3d

2.2.2 Light ray distribution

2.2.3 Light properties

2.2.4 Measurement precision changes

2.2.5 Image sensor properties

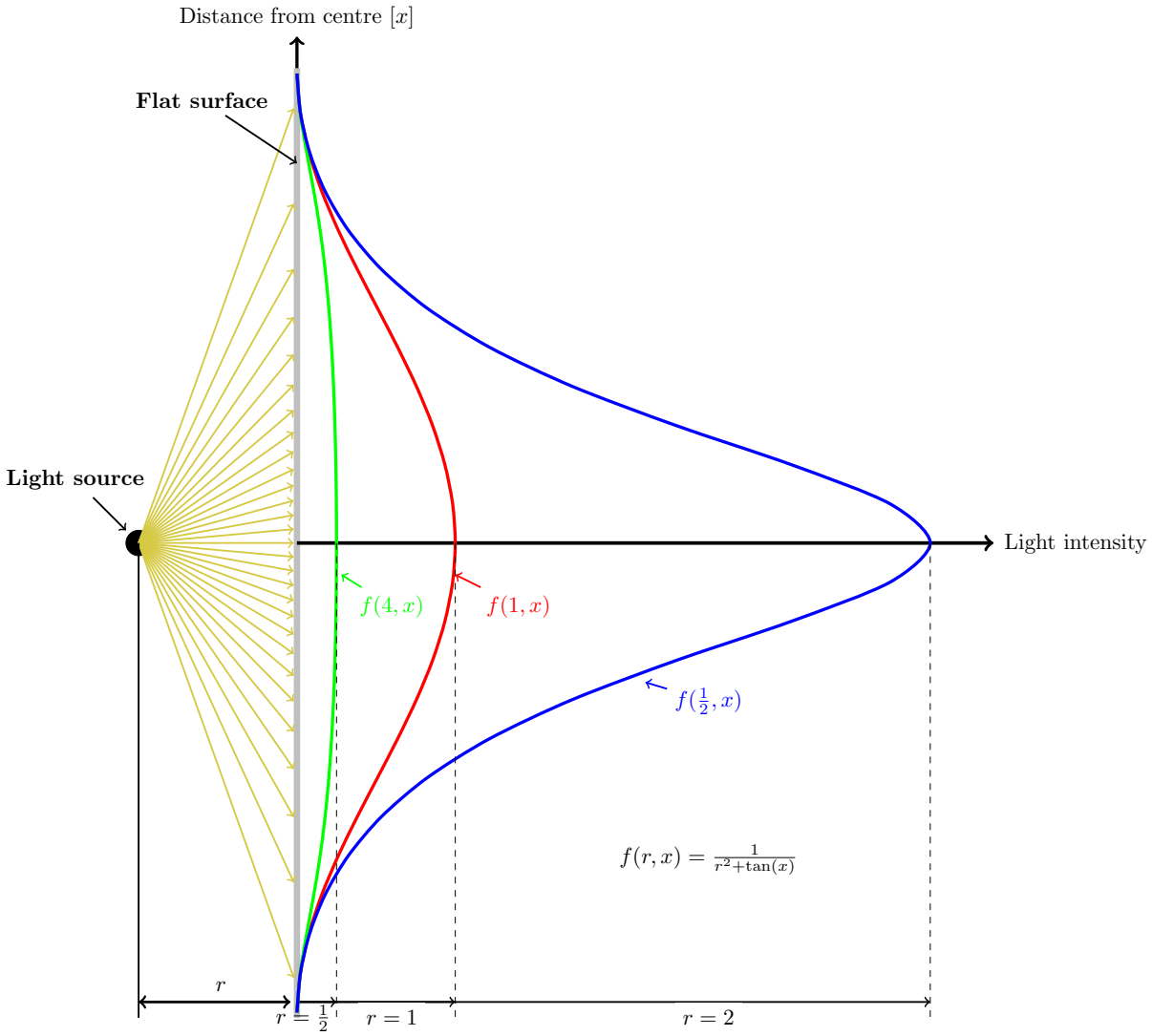

Figure 2.6: Light distribution

Chapter 3

Development

This chapter covers the developing process in more detail.

3.1 Calibration

This section focuses on the calibration of the Rasperry Pi Camera Module V2 (resolution set to 3280×2464 pixels), but all insights learned from these first attempts are applicable to the similar (but higher quality) cameras, which where later also used.

To capture the whole steel-spring, the camera has to be mounted approximately 250 mm away from it. From this distance, one pixel-width corresponds to a length within the tenths of a millimeter range. It is therefore absolutely necessary to calibrate the camera as described in section 2.1, since non-linear distortions can distort the image by 10-20 pixels or even more. Lens imperfections can therefore cause deviations in the measurement of several millimeters, which is not acceptable.

To calibrate a camera in OpenCV, one has to take images of a known 2D-pattern. It is reasonable to use a checkerboard, since OpenCV provides functions to detect checkerboard-corners reliably with subpixel precision.

3.1.1 How to obtain a usable calibration

First attempts to calibrate the camera failed. Despite reprojection errors of < 0.3 pixels, the obtained distortion coefficients did not seem to deliver a good undistortion of the image. Furthermore, new attempts with slightly different images of the checkerboard resulted in totally different coefficients.

It is therefore important to take a closer look at the technical aspects of the calibration process.

Calibration statistics

To get more insight what went wrong, some sort of statistics is needed. 200 images of the checkerboard from different view-points and angles has been taken. A couple of these images are shown in Figure 3.1

Randomly selected from these 200 are ten sets of each 20 images. Now is the camera calibrated separately with each set. To visualize the result, the difference from the distorted (real) and undistorted (corrected) on all locations of half the diagonal in the upper right quadrant

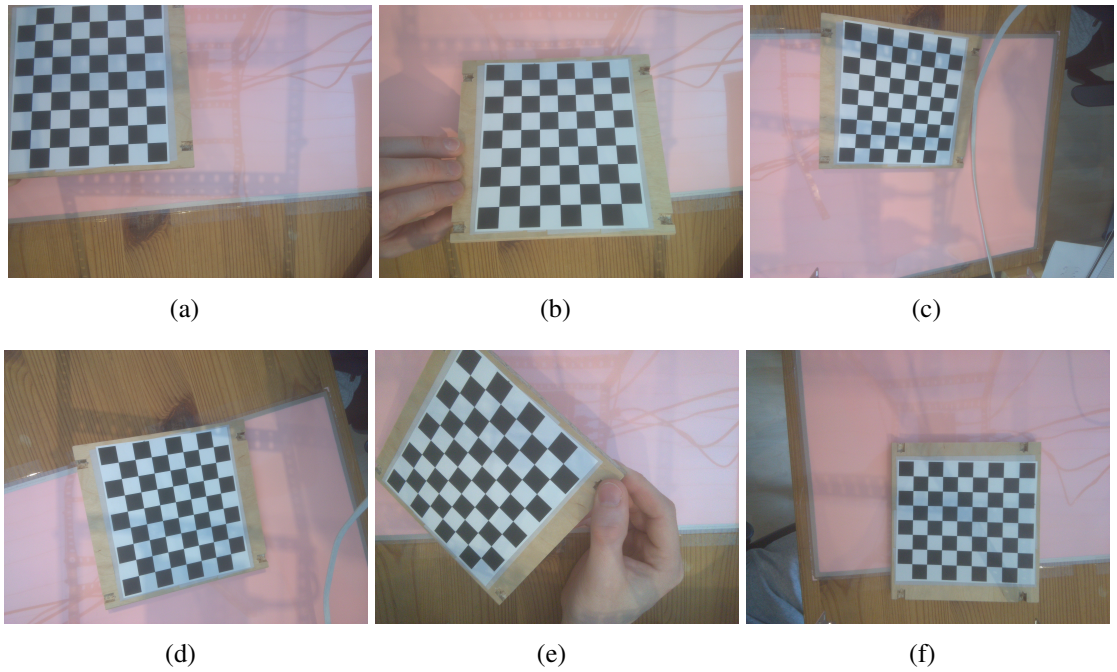

(a) (b) (c)

(d) (e) (f)

Figure 3.1: Some of the 200 images

of the image is plotted. In other words, we take a look at the distortion between the image center and the upper right corner (min to max radius). This plot is shown in Figure 3.2.

The distortion model introduces decentering effects and one could argue, that this plot should be made in all quadrants of the image. But since the decentering effects are rather small in comparison with the radial distortion which is symmetric with respect to the centerpoint it should be sufficient to plot only one quadrant. it is therefore assumed, that if the distortions are high in one quadrant, that the distortions in all other quadrants is also high and vice versa.

3.2 Software

3.3 Hardware

3.3.1 Demonstrator

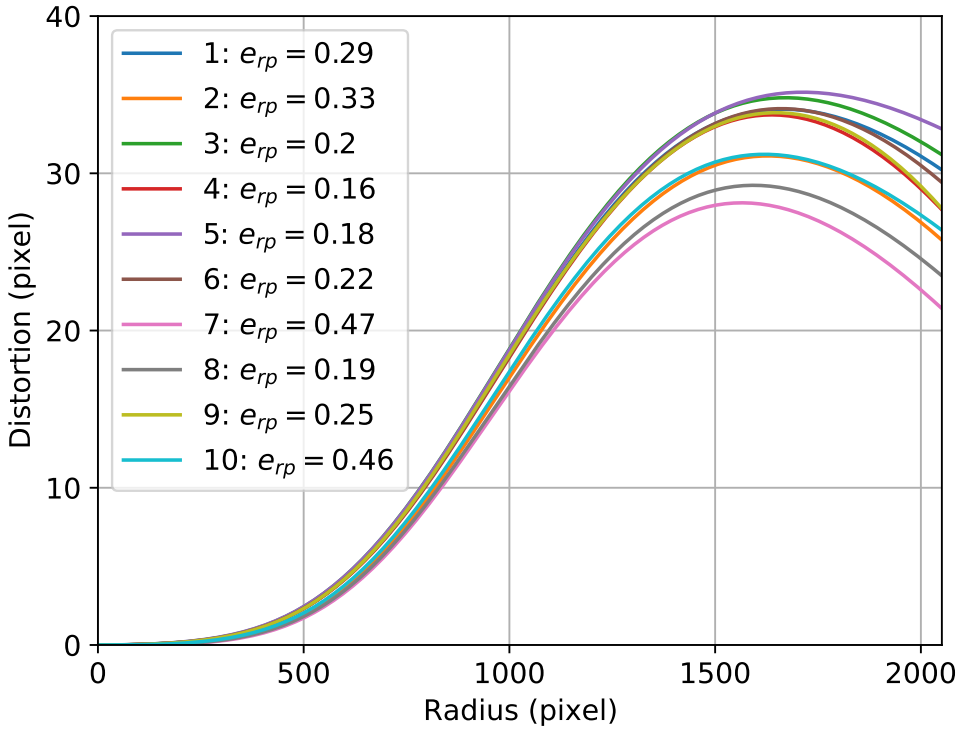

Figure 3.2: Distortion over the radius according to different sets if images

3.3.2 Back-light

The back-light developed for this project had following

3.3.3 Computer

3.3.4 Camera

The camera used for this project had to following evaluation criteria to meet:

- compatible with the Jetson Nano enviroment
- a good developer community
- open source drivers
- low cost
- minimum frame rate of 20[fps]
- measurement accuracy of $\frac{1}{10}$[mm]

The following is a list of the cameras that have been studied and used in the project:

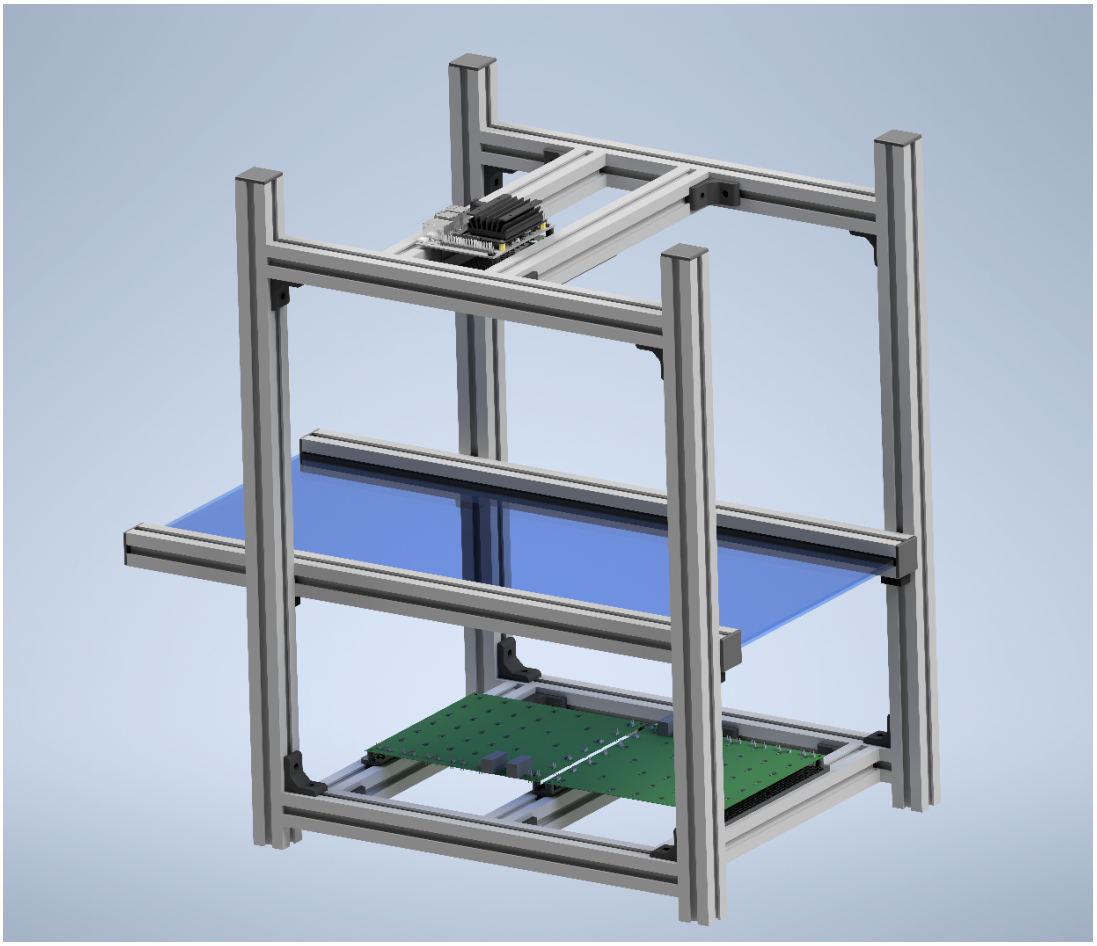

Figure 3.3: 3D-Model of the demonstrator

List of possible Cameras			
Company Camera Name	Raspberry Pi Camera Module V2	Raspberry Pi HQ Camera	Arducam Arducam IMX219 Low Distortion M12 Mount Camera Module
Price	$25	$50	$39.99
Camera Sensor	Sony IMX219	Sony IMX477	Sony IMX219
Still resolution	8M	12M	12.3M
Sensor resolution	3280 x 2464	4056 x 3040	3280 x 2464
Linux integration	V4L2 driver	V4L2 driver	V4L2 driver
Pixel size	1.12 x 1.12 μm	1.55 x 1.55μm	1.12 x 1.12 μm
Focal length	3.04[mm]	Depends on lens	2.8[mm]
Focal ratio	2.0	Depends on lens	2.8
View angle Horizontal	62.2 deg.	Depends on lens	75 deg.

3.3.5 Production cost

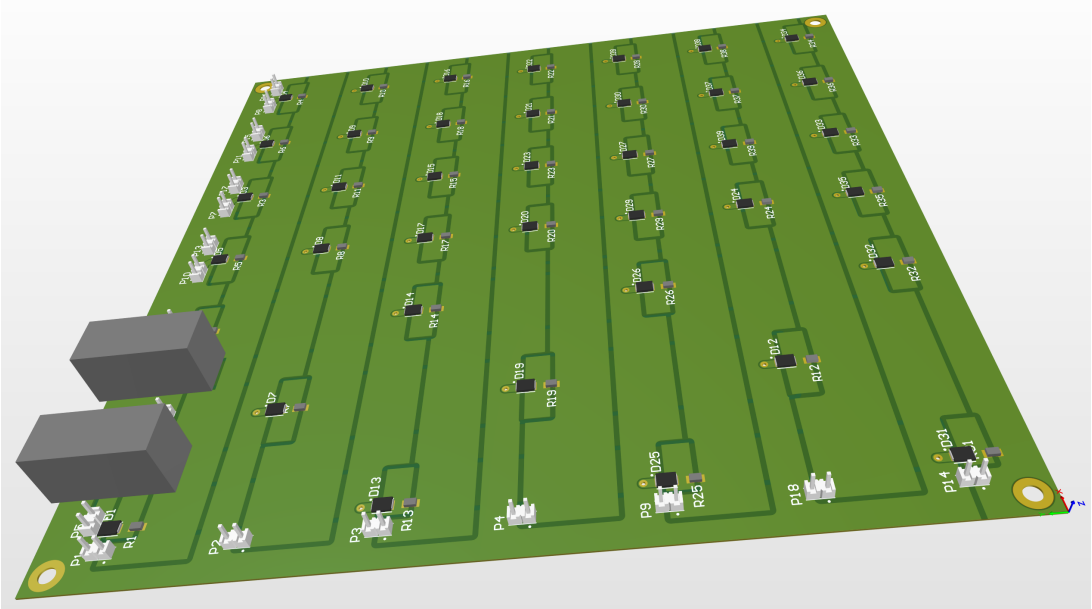

Figure 3.4: 3D-Model of the back-light PCB

Chapter 4

Results

This chapter covers the most important results.

Chapter 5

Conclusion

References

List of Figures

List of Tables

Statement of Plagiarism

We declare that, apart from properly referenced quotations, this report is our own work and contains no plagiarism; it has not been submitted previously for any other assessed unit on this or other degree courses.

Place	**Date**
Rapperswil	May 15, 2020

Signatures

Cedric Renda

Manuel Tischhauser

Appendix A

Requirements

A.1 Assignment

A.2 Requirement Specification